

# Supporting Information for: Mechanodelivery of nanoparticles to the cytoplasm of living cells

Nyssa T. Emerson, Chih-Hao Hsia\*, Ilona U. Rafalska-Metcalf, and Haw Yang<sup>†</sup>

*Princeton University, Princeton, New Jersey*

## Contents

<b>1</b>	<b>General data analysis and statistics</b>	<b>1</b>
<b>2</b>	<b>Materials</b>	<b>1</b>
<b>3</b>	<b>Determination of QD diameter by dynamic light scattering (DLS)</b>	<b>2</b>
<b>4</b>	<b>Passivation of QDs</b>	<b>4</b>
<b>5</b>	<b>Trypan blue quenching efficiency</b>	<b>6</b>
<b>6</b>	<b>Electroporation protocol used for viability comparison</b>	<b>8</b>
<b>7</b>	<b>Analysis of flow cytometry data</b>	<b>9</b>

---

\*Present address: Research Center for Applied Sciences, Academia Sinica, Nankang, Taipei, Taiwan.

<sup>†</sup>To whom correspondence should be addressed: hawyang@princeton.edu

## List of Figures

S1	Lognormal distributions of QD diameters determined by DLS. . . . .	3
S2	Emission spectra of QDs. . . . .	5
S3	Quenching efficiency of Trypan blue. . . . .	7
S4	FSC and SSC gating during flow cytometric analysis. . . . .	10
S5	Viability gating during flow cytometric analysis. . . . .	10
S6	Calculation of percent labeled cells during flow cytometric analysis. . . . .	10
S7	Calculation of loading efficiency during flow cytometric analysis. . . . .	11
S8	Close-ups of treated NIH/3T3 fibroblasts . . . . .	12
S9	Close-ups of treated WPE1-NB11 prostate epithelial cells . . . . .	13
S10	Additional fields of view of treated NIH/3T3 fibroblasts . . . . .	14
S11	Additional fields of view of treated WPE1-NB11 prostate epithelial cells . . . . .	15
S12	Treated NIH/3T3 fibroblasts 24 hours after passaging . . . . .	16
S13	Treated WPE1-NB11 prostate epithelial cells 24 hours after passaging . . . . .	17
S14	Additional images of nuclear targeting of NLS-QDs in NIH/3T3 fibroblasts. . . . .	18
S15	Additional images of nuclear targeting of NLS-QDs in WPE1-NB11 prostate epithelial cells. . . . .	19

# 1 General data analysis and statistics

All values are reported as mean  $\pm$  one standard deviation, calculated from a minimum of three separate experiments. In figures, error bars represent one standard deviation. When reported, statistical significance was determined by a Student's t-test in Matlab using the built-in `ttest` routine.

# 2 Materials

All materials were used as received without further purification. D-Penicillamine (DPA) was obtained from Acros Organics. Ethanolamine and 30–70 kDa poly-D-lysine hydrobromide were obtained from Sigma-Aldrich. Propidium iodide (PI, P3566), Hoechst 33342 (H3570), and tetramethylrhodamine dextran 70 kDa (TMR-Dextran, D1819) were obtained from Molecular Probes. Cell culture media, sera, Dulbecco's phosphate buffered saline with (DPBS++) and without (DPBS-) calcium and magnesium, Trypsin-EDTA (0.05% solution), trypan blue (0.4% solution), and Pluronic F-68 (PF-68, 10% solution) were obtained from Gibco. The His-NLS peptide used for nuclear targeting of QDs (sequence: NH<sub>2</sub>-HHHHHHSSDDEATADSQHSTPPKKKKRKV-COOH)<sup>1</sup> was synthesized by Genscript to a purity of > 98%.

### 3 Determination of QD diameter by dynamic light scattering (DLS)

QD diameter was measured by DLS with a 90-Plus particle sizer (Brookhaven Instruments). Organic phase QDs were diluted from hexane stock to  $\sim 800$  nM in toluene for analysis. Aqueous phase PEG-coated QDs were first extensively washed with 0.02-micron filtered (Anotop 10 Plus, Whatman) DPBS using an Ultra-0.5 ml 100 kDa MWCO centrifuge filter (Millipore). Washes were repeated (approximately 10–12 total) until the measured diameter was the same between two subsequent washes. Then washed QDs were diluted to a final concentration of 100–250 nM in 0.02-micron filtered DPBS for analysis. Autocorrelation functions were recorded in triplicate for 3 minutes. Fitting of the measured autocorrelation function and calculation of diffusion coefficient and particle diameter was performed automatically with built-in software (BI-MAS, Brookhaven Instruments); the refractive index of bulk CdSe ( $n_D = 2.5$ )<sup>2</sup> was used. Effective diameters of QDs in toluene and DPBS determined in this way are tabulated in Table S1. Representative plots of lognormal distributions of QDs in toluene and DPBS are shown in Figure S1. In the text QDs are referred to by the nominal diameter determined from DLS in organic phase.

sample name	ML ZnS	solvent	effective diameter (nm)	nominal diameter (nm)
7 nm QD	4	toluene	$7.2 \pm 0.8$	7
7 nm PEG-QD		DPBS	$27.4 \pm 1.0$	
10 nm QD	8	toluene	$10.5 \pm 0.2$	10
10 nm PEG-QD		DPBS	$28.9 \pm 3.5$	
15 nm QD	12	toluene	$14.7 \pm 0.1$	15
15 nm PEG-QD		DPBS	$33.9 \pm 0.6$	

**Table S1:** Effective diameter of size panel of QDs determined by DLS.

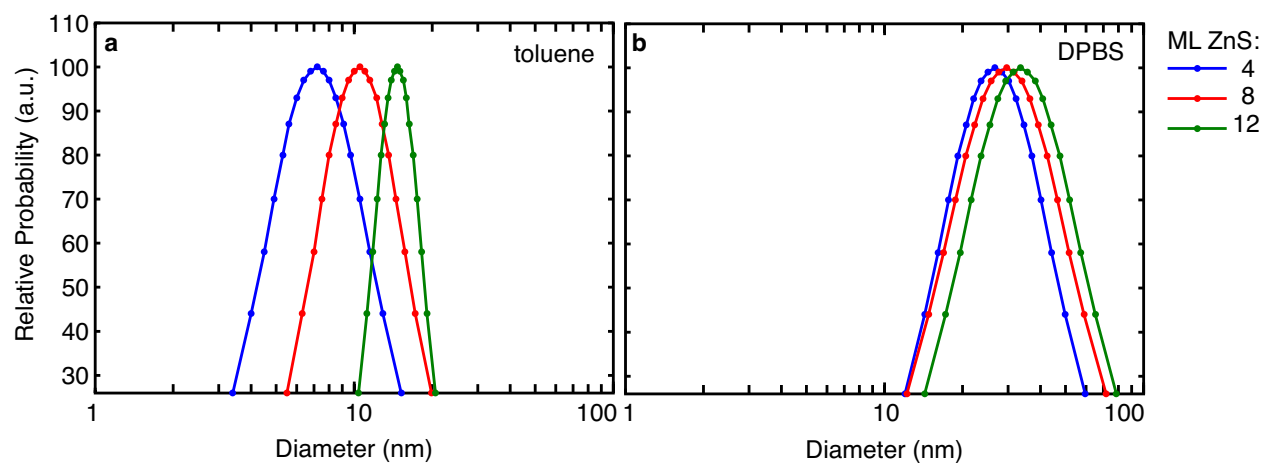


**Figure S1:** Representative lognormal distributions of QD diameters determined by DLS of (a) organic phase QDs in toluene and (b) aqueous phase PEG-coated QDs in DPBS. In these graphs, "a.u." stands for arbitrary units.

## 4 Passivation of QDs

Organic phase QDs were transferred to the aqueous phase by passivating with DPA following a previously reported procedure,<sup>3</sup> with minor alterations. Briefly, 1 nmol QDs in hexane were precipitated with acetone and pelleted by centrifugation. QDs were dispersed in 4.5 ml chloroform and 2 ml freshly prepared DPA solution (10% w/v DPA, 7% v/v ethanolamine in methanol) was added. The mixture was immediately vortexed, distributed evenly into five 1.5 ml tubes, and sonicated in a bath sonicator (VWR) for 1 hour or until QDs precipitated. Precipitated QDs were collected by centrifugation and resuspended in water, giving DPA-coated QDs.

DPA-coated QDs were then passivated with a dithiol poly(ethylene glycol) (PEG) ligand (lipoamide-dPEG12, Product # 10801, Quantabiodesign). The dithiol group confers additional colloidal stability and the long PEG group confers resistance to nonspecific adsorption.<sup>4</sup> 2.5 equivalents of NaBH<sub>4</sub> were added to 1 ml 10 mM lipoamide-dPEG12 and the solution was incubated for 10 minutes to reduce the dithiol bond. This reduced ligand stock was added to 1 nmol, 0.5 nmol, or 0.25 nmol DPA-coated 7, 10, or 15 nm QDs, respectively, diluted into 9 ml of 50 mM borate buffer, pH 8.3. The mixture was protected from light and tumbled overnight (>12 hours). The resulting PEG-coated QDs were then washed and concentrated to ~4  $\mu$ M with a 50 kDa MWCO ultracentrifugal filter (Millipore) into borate buffer and subsequently used for experiments. Representative emission spectra (Fluorolog-3, Jobin Yvon) of PEG-coated 7, 10 and 15 nm QDs are shown in Figure S2.

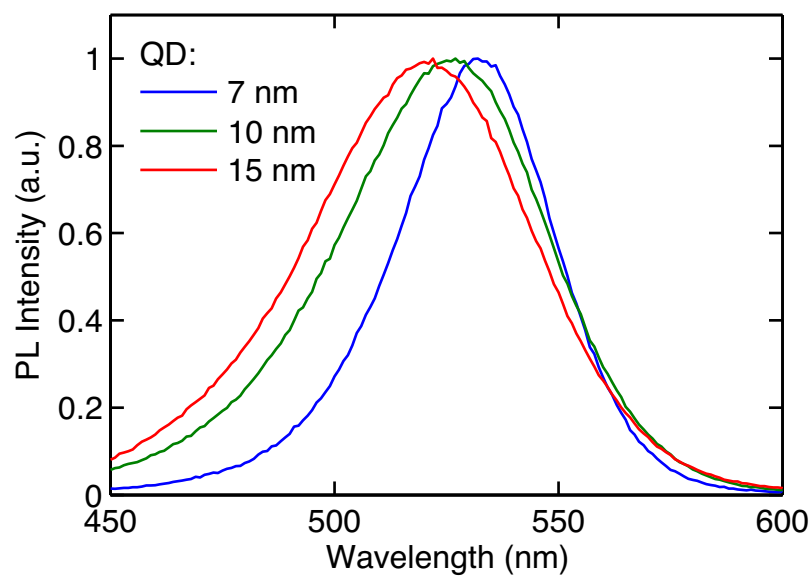


**Figure S2:** Representative emission spectra of PEG-coated 7, 10, and 15 nm QDs, which were used for loading experiments, in water. Excitation wavelength was 405 nm.

## 5 Trypan blue quenching efficiency

To determine quenching efficiency, QD emission intensity was measured at 525 nm (405 nm excitation) with a Spectramax M5 plate reader (Molecular Devices) using commercial software (SoftMaxPro, Molecular Devices) before and after trypan blue addition. 90  $\mu$ l of 5, 10, or 50 nM PEG-coated 15 nm-QDs in DPBS was aliquoted in each of 6 wells of a 96-well microtiter plate (Grenier). Initial emission intensity was recorded for each well, and background from DPBS alone was subtracted. Next, 90  $\mu$ l of 4000, 400, 40, 4, 0.4, or 0  $\mu$ g/ml trypan blue in DPBS was added to each well and solutions were mixed by pipetting. Final emission intensity was recorded for each well, and background from trypan blue added to DPBS alone was subtracted.

Quenching efficiency ( $QE$ ) was calculated as

$$QE (\%) = 100 \times \left( 1 - \frac{1}{N_0} \frac{I_f}{I_i} \right),$$

where  $I_f$  and  $I_i$  are the final and initial background-corrected emission intensities, respectively.  $N_0$  is a normalization factor, defined as  $N_0 = I_f^0/I_i^0$ , the relative change in emission on adding only DPBS to the QDs. This was included to account for effects of *e.g.* dilution on the change of emission intensity. Figure S3 shows the measured quenching efficiency of trypan blue for three QD concentrations. Data points are mean  $\pm$  standard deviation for three separate experiments.



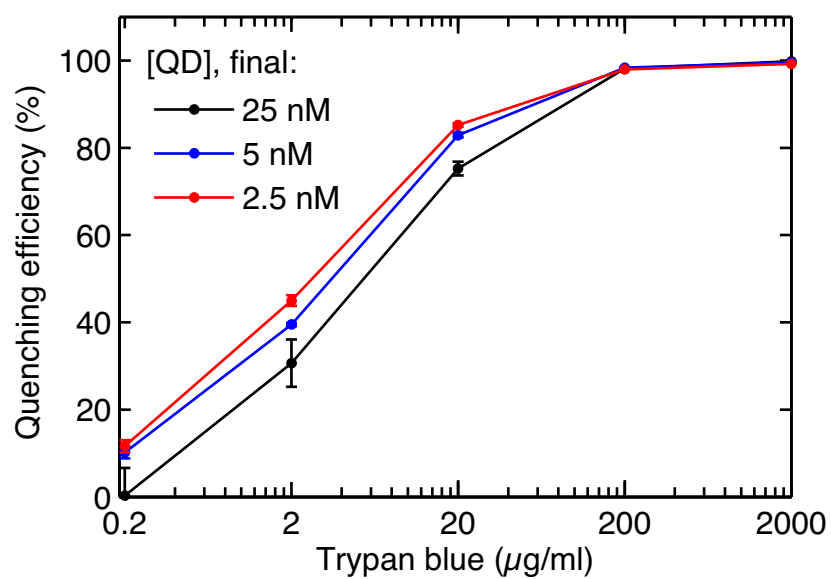


**Figure S3:** Quenching efficiency of trypan blue, calculated at three QD concentrations as described in the text.

## **6 Electroporation protocol used for viability comparison**

NIH/3T3 fibroblasts were cultured in 100 mm dishes until 80% confluence. Cells were detached by trypsin and resuspended in complete medium to a concentration of  $6-7 \times 10^6$  cells/ml. 300  $\mu$ l cell suspension was combined with 100  $\mu$ l of 2  $\mu$ M QDs in a 4 mm electroporation cuvette (Eppendorf) and placed on ice for 7 minutes to minimize endocytic uptake. The cuvette was then subjected to electroporation (GenePulser XCell, BioRad) following an exponential decay pulse protocol with voltage and capacitance held at 220 V and 950  $\mu$ F, respectively. A typical time-constant for exponential decay was 40–50 ms. After pulse application, cuvettes were returned to ice for 3 minutes. Cells were then collected with 1 ml complete medium, washed twice with 2% fetal bovine serum in DPBS-- (2% FBS) and resuspended into 1 ml 2% FBS for analysis on the flow cytometer.

## 7 Analysis of flow cytometry data

Flow cytometry data was analyzed with a commercial software package (FlowJo). All samples were first gated on forward and side scatter to exclude debris (Figure S4). To calculate viability, a conservative gate for live cells based on PI intensity was designated from a control population and applied to all samples (Figure S5). To determine the percent of cells labeled with QDs or TMR-Dextran, positive gates were designated to include cells which exhibited fluorescence or PL intensity greater than 99% of the untreated population (Figure S6). To determine efficiency of QD labeling, quadrant gates were designated to exclude 99% of the untreated population from quadrants I, II, and IV (Figure S7). The efficiency of QD labeling was then calculated as

$$\text{Loading efficiency} = \frac{\# \text{ of cells in QIII}}{\# \text{ of cells in QI} + \# \text{ of cells in QIII}} \times 100.$$

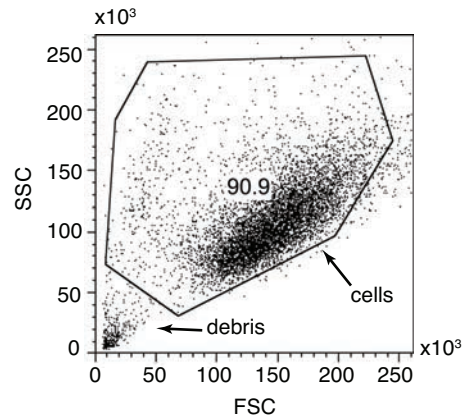


**Figure S4:** Example of gating for cells based on forward (FSC) and side (SSC) scatter, which was performed on all samples. A representative two parameter scatter plot of a control population showing this gate is shown.

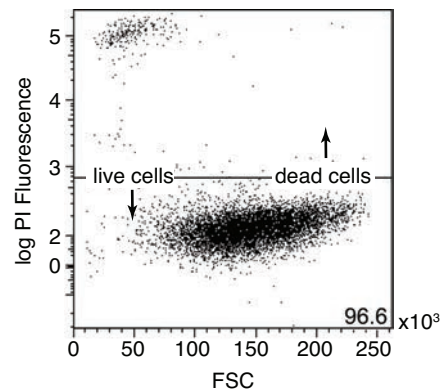


**Figure S5:** Live and dead cell gates used for calculation of viability, based on propidium iodide (PI) fluorescence intensity. A control population is shown.

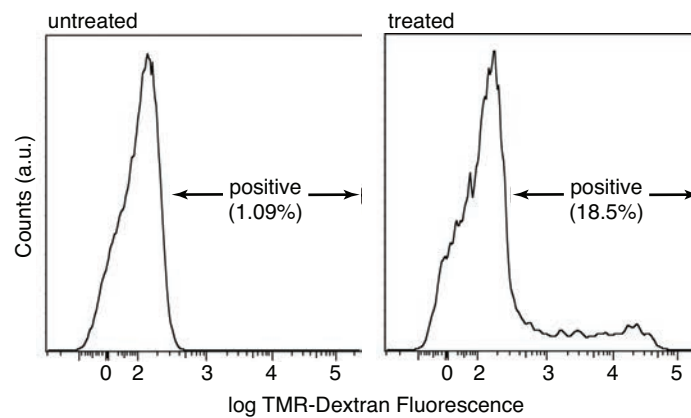


**Figure S6:** Calculation of percent labeled cells. Those cells with fluorescence intensity greater than 99% of the untreated population (left) were considered positively labeled. TMR-Dextran labeling is shown.

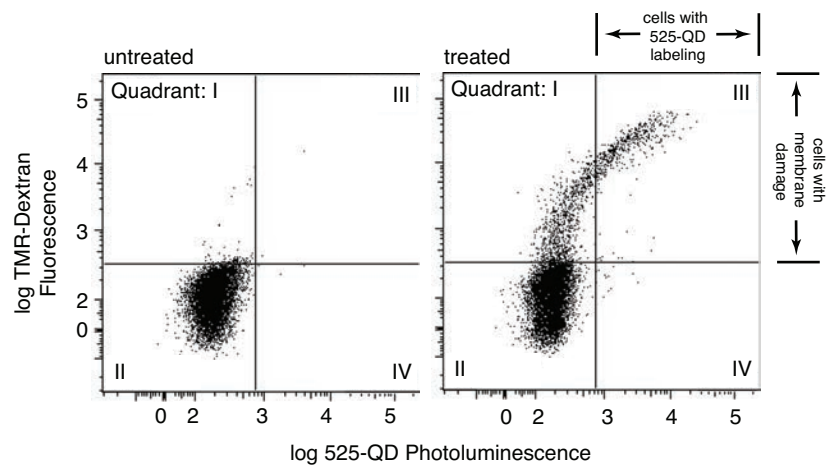


**Figure S7:** Calculation of loading efficiency of QDs based on simultaneous labeling with QDs and TMR-Dextran. Quadrant gates were designated to exclude 99% of the untreated population from quadrants I, III, and IV.

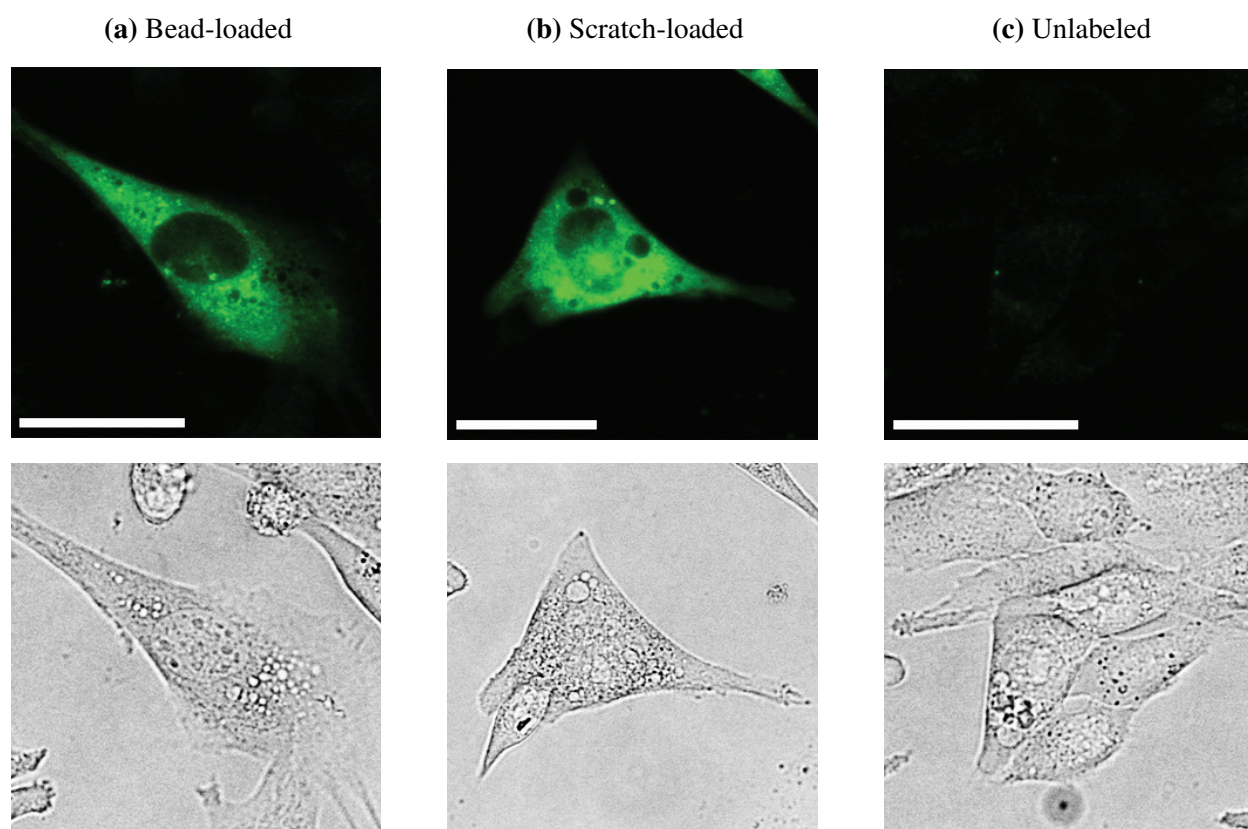


**Figure S8:** Close-ups of NIH/3T3 fibroblasts subjected to different treatments to show diffuse cytoplasmic labeling. Cells were bead-loaded (left) or scratch-loaded (middle) with 1  $\mu\text{M}$  10 nm-QDs. A subset of unlabeled cells from the scratch-loaded sample is shown for comparison (right). The bead-loaded cells is the same image as from the main text (Figure 2e). False color epifluorescence (top) and brightfield (bottom) images were acquired two hours after treatment. Trypan blue was included in the imaging medium at 40  $\mu\text{g/ml}$ . All images were acquired and adjusted identically. Scale bars are 50  $\mu\text{m}$ .

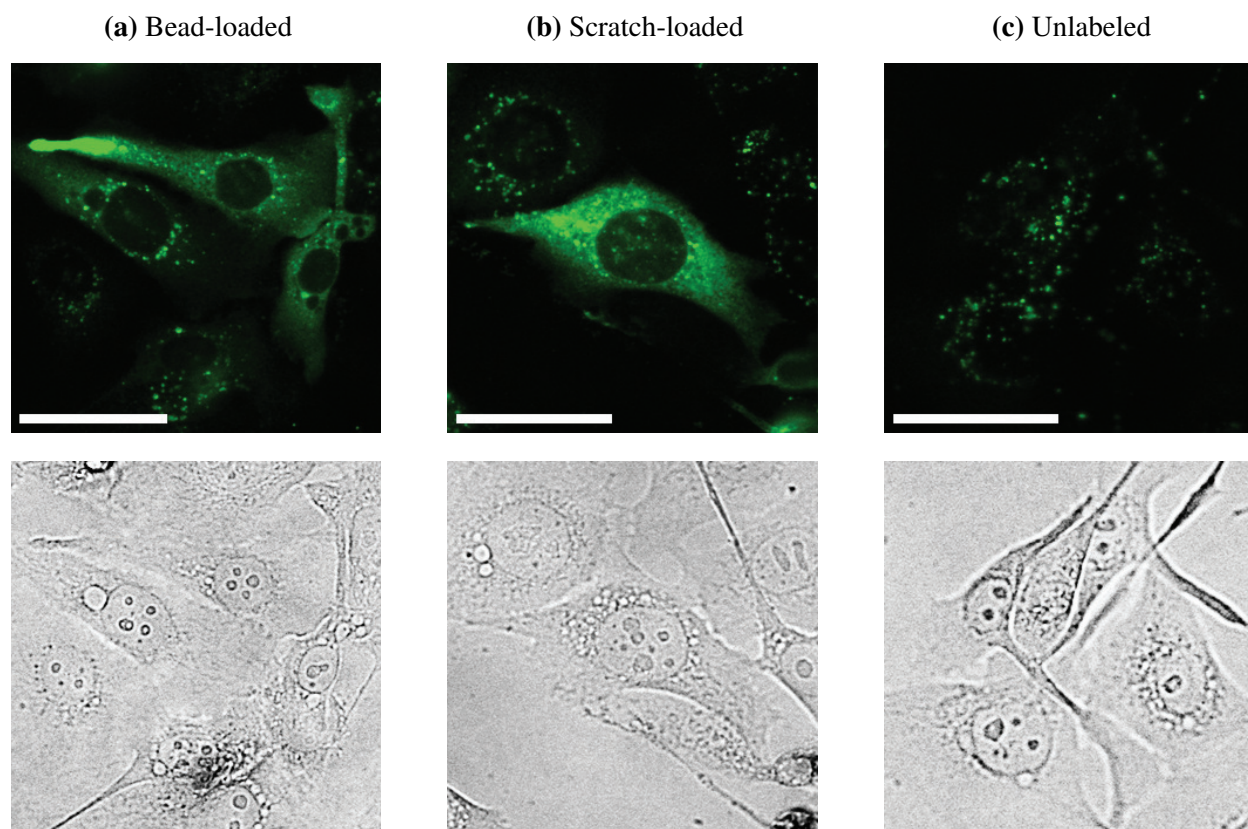


**Figure S9:** Close-ups of WPE1-NB11 prostate epithelial cells subjected to different treatments to show diffuse cytoplasmic labeling. Cells were bead-loaded (left) or scratch-loaded (middle) with 1  $\mu\text{M}$  10 nm-QDs. A subset of unlabeled cells from the scratch-loaded sample is shown for comparison (right). False color epifluorescence (top) and brightfield (bottom) images were acquired two hours after treatment. Trypan blue was included in the imaging medium at 40  $\mu\text{g/ml}$ . All images were acquired and adjusted identically. Scale bars are 50  $\mu\text{m}$ .



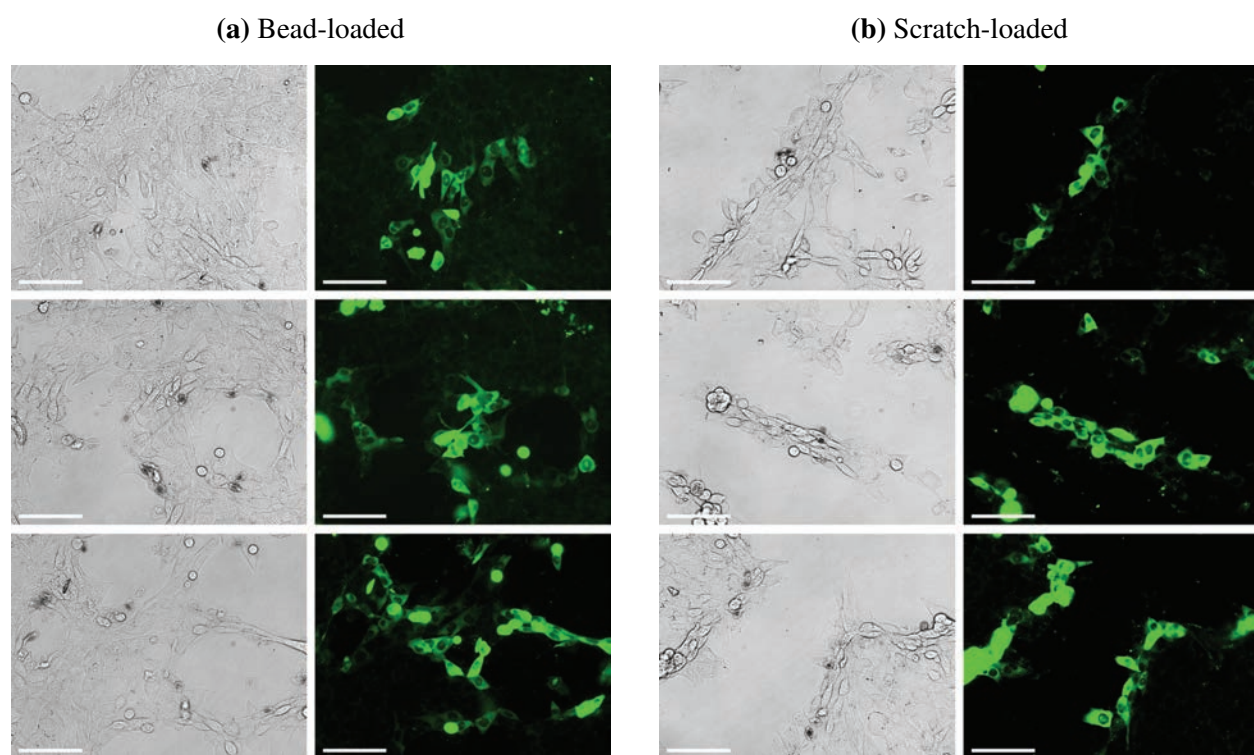


**Figure S10:** Additional fields of view of treated NIH/3T3 fibroblasts demonstrating the extent of QD labeling. Fibroblasts were treated as indicated with 1  $\mu\text{M}$  10 nm-QDs. Brightfield (left) and false color epifluorescence (right) images were acquired two hours after treatment. Trypan blue was included in the imaging medium at 40  $\mu\text{g/ml}$ . Scale bars are 100  $\mu\text{m}$ .



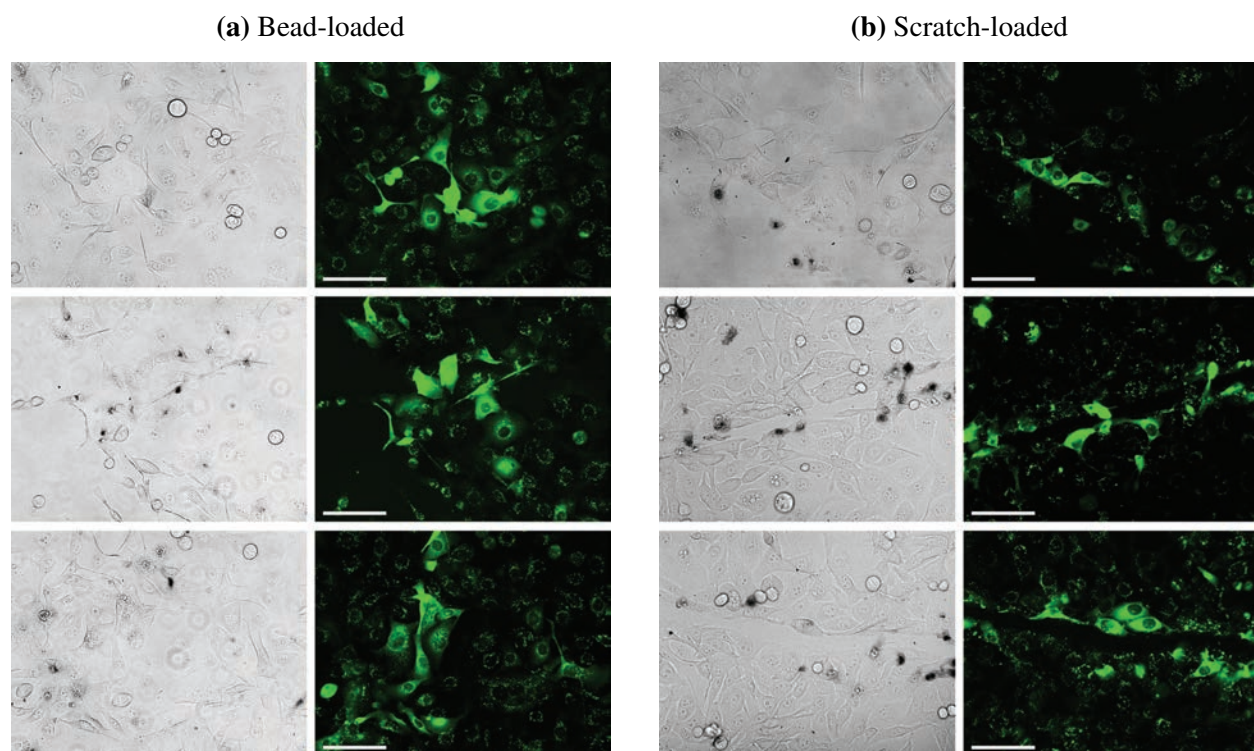


**Figure S11:** Additional fields of view of treated WPE1-NB11 prostate epithelial cells demonstrating the extent of QD labeling. Cells were treated as indicated with 1  $\mu\text{M}$  10 nm-QDs. Brightfield (left) and false color epifluorescence (right) images were acquired two hours after treatment. Trypan blue was included in the imaging medium at 40  $\mu\text{g/ml}$ . Dead cells have black stained nuclei. Scale bars are 100  $\mu\text{m}$ .

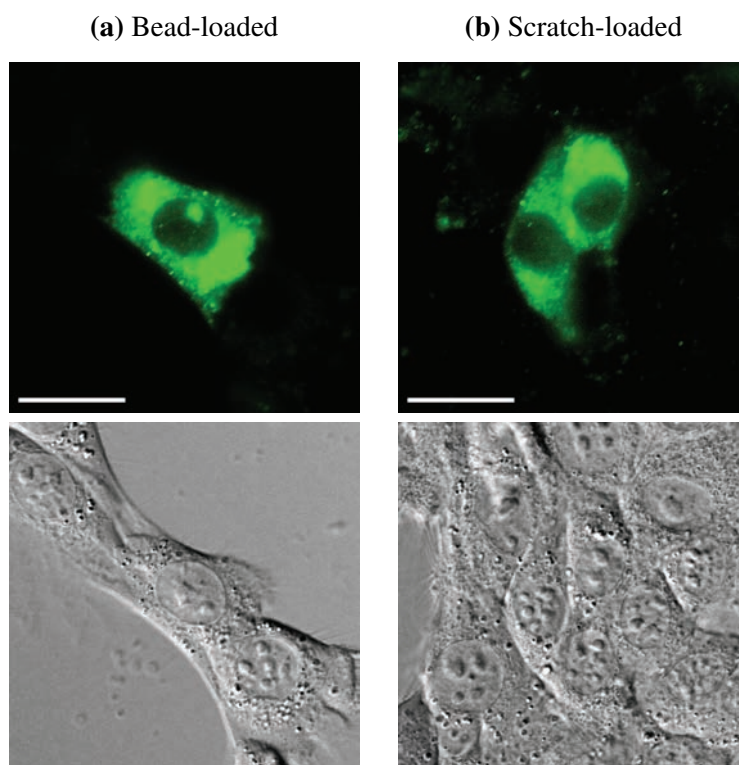


**Figure S12:** Representative false color epifluorescence (top) and DIC (bottom) images of treated NIH/3T3 fibroblasts which retained QD labeling after passaging. Cells were treated as indicated with 1  $\mu$ M 10 nm-QDs, briefly recovered, and then trypsinized and replated on a fresh coverslip as if to passage. Images were acquired 24 hours later. Observation of QD-labeled cells after passaging suggests that QDs are indeed present in the cytoplasm, and furthermore, that QD delivery does not adversely affect viability. Scale bars are 50  $\mu$ m.

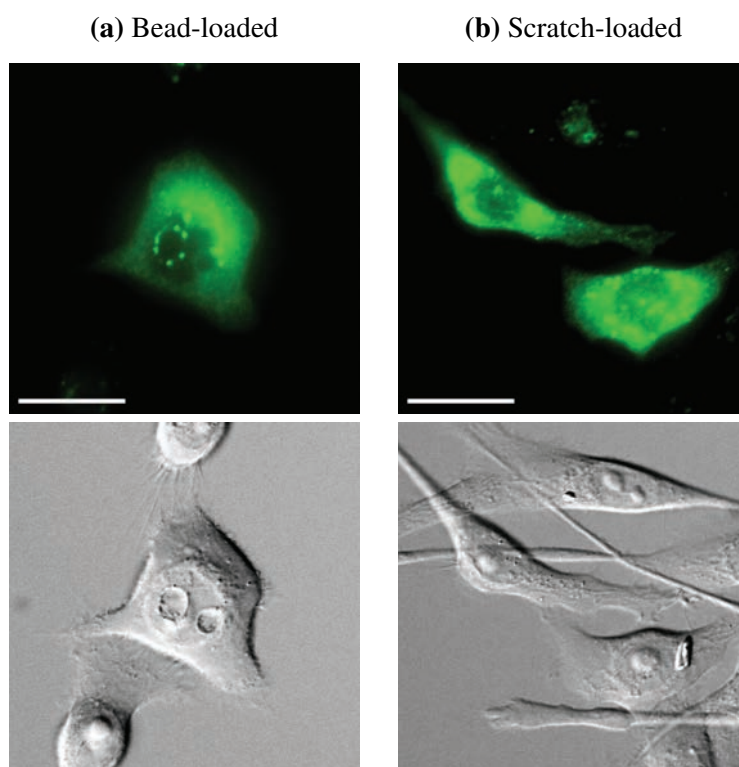


**Figure S13:** Representative false color epifluorescence (top) and DIC (bottom) images of treated WPE1-NB11 prostate epithelial cells which retained QD-labeling after passaging. Cells were treated and imaged as described in Figure S12. Scale bars are 50  $\mu\text{m}$ .

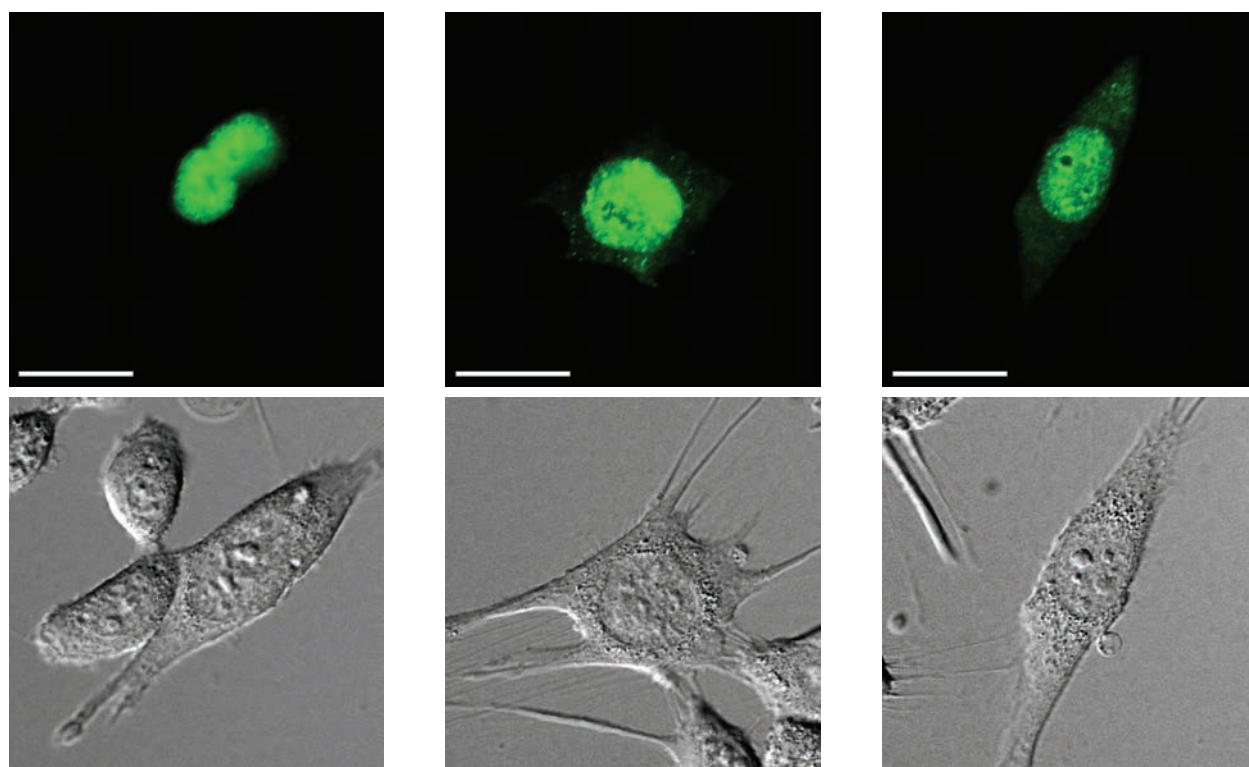


**Figure S14:** Additional false color epifluorescence (top) and DIC (bottom) images of NIH/3T3 fibroblasts subjected to bead-loading with 1  $\mu$ M NLS-QDs. Images were acquired three hours after treatment. Cells clearly exhibit nuclear labeling. Scale bars are 50  $\mu$ m.

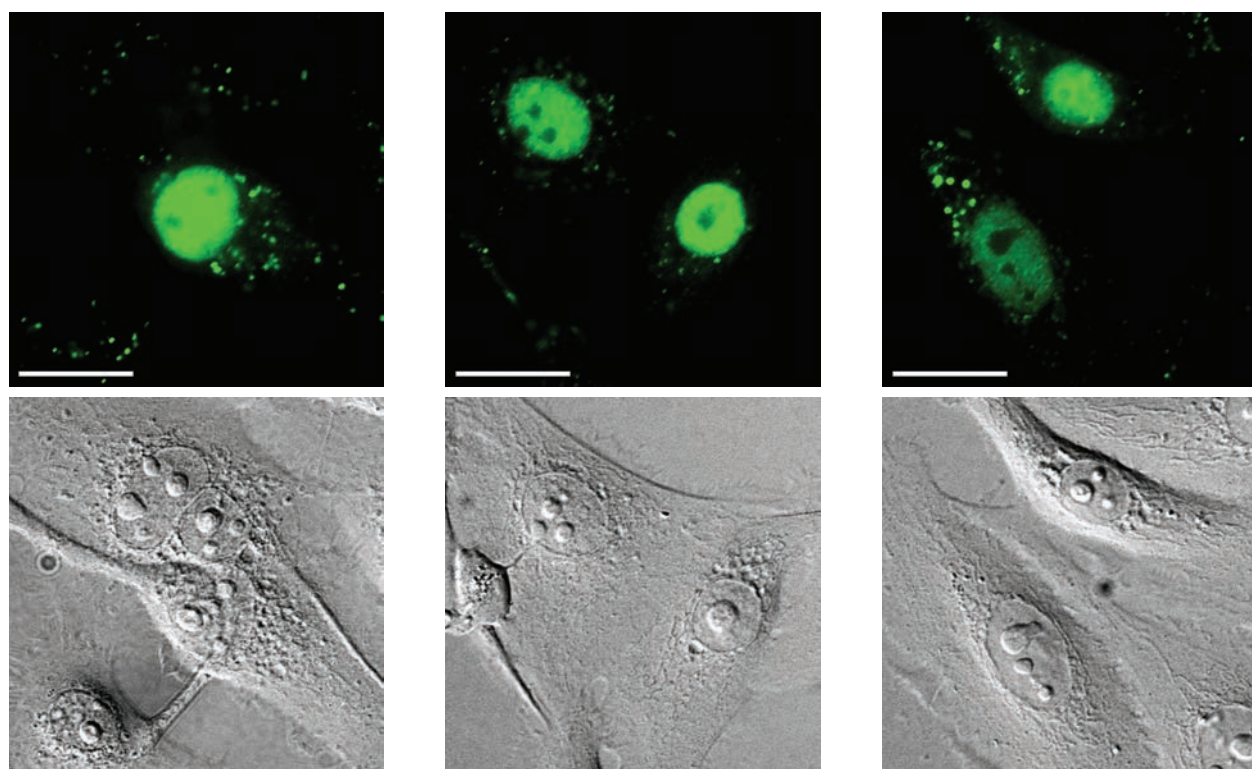


**Figure S15:** Additional false color epifluorescence (top) and DIC (bottom) images of WPE1-NB11 prostate epithelial cells subjected to scratch loading with 1  $\mu$ M NLS-QDs. Images were acquired three hours after treatment. Cells clearly exhibit nuclear labeling. Scale bars are 50  $\mu$ m.

## References

1. Derfus, A. M., Chan, W. C. W., and Bhatia, S. N. (2004) Intracellular delivery of quantum dots for live cell labeling and organelle tracking. *Adv. Mater.* *16*, 961–966.
2. Jensen, B., and Torabi, A. (1986) Refractive index of hexagonal II-VI compounds CdSe, CdS, and  $\text{CdSe}_x\text{S}_{1-x}$ . *J. Opt. Soc. Am. B* *3*, 857–863.
3. Hsia, C.-H., Wuttig, A., and Yang, H. (2011) An Accessible Approach to Preparing Water-Soluble  $\text{Mn}^{2+}$ -Doped (CdSSe)ZnS Core(Shell) Nanocrystals for Ratiometric Temperature Sensing. *ACS Nano* *5*, 9511–9522.
4. Mei, B. C., Susumu, K., Medintz, I. L., Delehanty, J. B., Mountziaris, T. J., and Mattoussi, H. (2008) *J. Mater. Chem.* *18*, 4949–4958.